Z. Phys. Chem. **221** (2007) 785–799 / **DOI** 10.1524/zpch.2007.221.6.785

Hydrophobic Interactions of Xenon by Monte Carlo Simulations

By Orkid Coskuner[1] and Ulrich K. Deiters*

[1] National Institute of Standards and Technology, Physical and Chemical Properties Division, 100 Bureau Drive, Mail Stop 8380, Gaithersburg, MD 20889, USA
[2] Institute of Physical Chemistry, University of Cologne, Luxemburger Str. 116, D-50939 Köln, Germany

(Received November 24, 2006; accepted February 27, 2007)

Xenon / Hydrophobic Interactions / Chemical Potential / Water / Monte Carlo Simulation

Hydrophobic interactions of xenon atoms dissolved in liquid water were studied by NpT Monte Carlo simulations in the temperature range 298.15 to 333 K and at ambient pressure. Structural properties of dilute xenon solutions were calculated and compared to those of bulk water in order to show the influence of the hydrophobic solute. It was found that the xenon atoms tend to aggregate with increasing temperature. At low temperatures the aggregates are predominantly solvent-separated pairs; at higher temperatures the *quota* of contact pairs increases. Furthermore, the residual chemical potentials of xenon and water were calculated with different methods; it was found that the Widom insertion methods works best for this system. For the thermodynamic conditions of this work, the residual chemical potential of water in the presence of xenon was found to be a linear function of temperature.

1. Introduction

The unusual thermophysical properties of dilute solutions of nonpolar substances in water have been studied since many decades by experimentalists as well as theoreticians. They are usually explained with so-called "hydrophobic interactions" – special interactions between two or more nonpolar solute molecules in water, solute interactions with water molecules, and interactions between water molecules in the vicinity of these solutes. One of the peculiarities often observed with nonpolar solute molecules in water is their tendency to aggregate – even if the solute–solute pair potential is rather weak. Hydrophobic association is evidently caused by statistical, solvent-related forces.

* Corresponding author. E-mail: ulrich.deiters@uni-koeln.de

Consequently there have been many attempts to explain hydrophobic effects quantitatively by means of statistical thermodynamics or computer simulation. The simulations were mostly based on molecular dynamics simulations and provided valuable insights into the nature of the hydrophobic interactions; an important result is that the nonpolar molecules can either form contact pairs or solvent-separated pairs. The approximate integral equation by Pratt and Chandler was the first theory that demonstrated the importance of solvent-separated solute pairs in hydrophobic interactions [1].

While hydrophobic interactions of small alkanes, especially methane and ethane, have been studied extensively, relatively few publications deal with hydrophobic interactions of inert gases. An example is the work of Paschek, who studied solutions of xenon in water and discussed the influence of the water pair potential model on the structural and thermodynamic properties of water in the vicinity of dissolved xenon [2]. The hydration properties of xenon in water were also studied by Tanaka and Nakanishi [3], who computed enthalpy and chemical potential values for xenon in water from Monte Carlo simulations. According to their studies, the structural properties of water in the vicinity of a xenon atom differ from those of bulk water.

Straatsma *et al.* performed molecular dynamics calculations for water and used two different methods – perturbation theory and thermodynamic integration – to obtain the Gibbs energy required to create a cavity and to insert a noble gas atom into it. They found a significant difference between the values for neon and xenon, and attributed it to a size-induced structure change in the water layers surrounding the cavities [4].

De Souza and Ben-Amotz correlated the attractive solvation energy with the polarizability of the solute, using a hard-fluid model, and concluded that the small size of water molecules is even more important for the understanding of hydrophobic solvation than the hydrogen-bonding pattern of water [5]. Still, collective motions and energy fluctuations associated with hydrogen-bond network rearrangements contribute significantly to the solubility of inert gases in water [6].

Recently, Graziano investigated the hydration properties of xenon in water, using a scaled-particle theory based on the assumption that both solute and solvent particles can be modelled as spheres [7]. His studies showed the importance of hydrogen bonding capabilities of various solvents for the solvation of xenon.

In spite of insights gained from computer simulations, neither the effect of temperature on the hydrophobic interactions between xenon atoms in water nor the influence of xenon atoms on the water structure are quite clear. It is generally believed that the presence of a nonpolar solute increases the degree of hydrogen bonding in the first solvation shell [8], an effect that is often referred to as the “iceberg hypothesis” [9]. The number of water molecules in the first hydration shell is another key property for the understanding of hydrophobic interactions [8, 10].

Because of the strong influence of the water interaction potential on the outcome of theoretical studies of hydrophobic effects [2], much effort went into the development of model potentials with which liquid water could be simulated accurately. Earlier published potential functions for water include those of Popkie *et al.* [11] and of Stillinger and Rahman [12]. For quantitative modelling of water and water solutions especially the SPC and SPCE models of Berendsen *et al.* [13, 14] and the transferable interaction potentials of Jorgensen and coworkers proved very useful; especially the transferable interaction potentials (TIP*n*P) have been widely used in molecular simulations of water [15–17].

One of the best tests of the quality of water models is their ability to represent the density–temperature relation of liquid water (for which experimental data of high accuracy are available). Here it turns out that, except for the five-site transferable intermolecular potential function (TIP5P) model proposed by Mahoney and Jorgensen [17], none of the earlier models can reproduce the well-known density maximum at about 277 K and at normal pressure. The TIP5P model was also reported to be able to accurately reproduce the experimental value of the density of liquid water at room temperature, $0.997\,g/cm^3$. However, recent simulations in which the long range interactions were treated with the Ewald sum method yielded slightly smaller densities for TIP5P water [2, 18]. Moreover, Paschek was able to reproduce the accepted density values at various temperatures for TIP4P and SPCE water, but not for TIP5P water. Recently we presented a modified TIP5P model for water based on *ab initio* calculations [19]. This water model yields more accurate thermodynamic properties such as density and chemical potential between 298.15 and 318 K at normal pressure.

In this work we present a study of the hydrophobic interactions of xenon in liquid water by means of Monte Carlo simulations, utilizing various water interaction potentials, namely SPCE [14], original TIP5P [17], and modified TIP5P [19]. Structural and thermodynamic data are reported in the temperature range 298.15 to 333 K and compared with simulation data of bulk water; several different methods were used to obtain the residual chemical potentials of water and xenon. The simulation results are analyzed in order to show the association of xenon atoms and its temperature dependence.

2. Methods

The SPCE [14], the original TIP5P [17], and a modified TIP5P [19] potential function for water were chosen for studying the influence of these models on the hydrophobic interactions of xenon atoms dissolved in liquid water. The SPCE potential function is a three-center point charge potential function for water and includes a self-energy correction term with a reparametrization of the SPC (simple point charge) model for water [13]. The original and modi-

Table 1. Lennard–Jones potential parameters and partial charges describing the water–water and xenon–xenon pair interactions. The xenon-water cross parameters are calculated from the Lorentz–Berthelot combining rules Eq. (1).

model	σ/Å	ϵ/kJ mol^{-1}	q_{H}/e
SPCE	3.166	0.650	0.42348
orig. TIP5P	3.120	0.669	0.241
mod. TIP5P	3.117	0.669	0.239
xenon	3.975	1.785	0.000

fied TIP5P models for water consist of a Lennard–Jones center representing the oxygen atom, two equal positive point charges representing the two hydrogen atoms, and two negative point charges for the lone electron pairs; the point charges form a distorted tetrahedron [17, 19]. The parameters of these water models as well as the Lennard–Jones potential parameters used for the representation of xenon are given in Table 1. It should be noted that the xenon parameters used in this work were fitted to pure component properties only [20].

Lorentz–Berthelot combining rules were used for the water-xenon cross terms,

$$\sigma = \frac{1}{2}(\sigma_{\mathrm{AA}} + \sigma_{\mathrm{BB}})$$
$$\epsilon_{\mathrm{AB}} = (\epsilon_{\mathrm{AA}}\epsilon_{\mathrm{BB}})^{1/2}\,, \tag{1}$$

where A and B stand for water and xenon, respectively.

The simulations were carried out with an isobaric–isothermal ensemble Monte Carlo program, HYDRO [19]. The program uses periodic boundary conditions, the minimum image convention, and Metropolis criteria for acceptance or rejection of trial configurations. Coulombic interactions were taken into account with the Ewald sum method [21, 22], using conducting boundary conditions, a screening parameter of $6/L$ (L: simulation box length, a fluctuating property during the simulation), and a Fourier space vector of $\boldsymbol{k} = 10\pi/L$. From these Monte Carlo simulations the site–site radial distribution functions, density, enthalpy, and residual chemical potentials of water and xenon were obtained.

The lack of a corresponding microscopic analogue, *i.e.*, a function of configuration space variables to be averaged to obtain the accurate results, constitutes the principal difficulty in calculations of chemical potentials and related properties (*e.g.*, Gibbs energy, entropy) calculations. Various methods have been developed for determination of the chemical potential by computer simulation, such as particle insertion and deletion methods, or perturbation methods. We calculated the residual chemical potential of xenon with three different methods: the Widom insertion scheme [23], the

Widom deletion scheme [24, 25], and the two-step particle deletion scheme of Boulougouris *et al.* [26]. For the first method a test particle is added to the simulation ensemble with N particles, and resulting energy change is recorded. The Widom deletion method is based on the comparison of the free energies of ensembles with N and $N-1$ particles. The particle deletion scheme of Boulougouris *et al.* is similar to the Widom deletion method, but in an intermediate step replaces the particle to be removed by a hard sphere, in order to avoid the bias that is caused by the remaining hole when a particle is simply deleted.

The particle deletion scheme of Boulougouris *et al.* is known to work well for spherical particles, but was recently shown to yield larger deviations from the experimental values than the Widom insertion method in simulations of water using the original or the modified TIP5P potential functions [19].

Simulation runs for hydrophobic interactions were performed with 216 water molecules and 2 xenon atoms. A real cut-off of 10 Å was applied to short range interactions, with long range corrections for larger distances. The simulations consisted of 2.5×10^6 equilibration moves, followed by 9×10^6 production moves. Block average analysis was used to determine the statistical uncertainty, where each run was subdivided into 100 blocks.

Coordination numbers were calculated as integrals over the pair correlation functions,

$$N_c = 4\pi\rho \int_0^{r_{min}} r^2 g(r)\, dr\,, \tag{2}$$

where ρ is the number density at given temperature and pressure.

3. Results and discussion

Figure 1 shows simulated oxygen–oxygen radial distribution functions $g_{OO}(r)$ of a liquid xenon-water solution at a mole fraction $x_{Xe} = \frac{2}{218} = 0.00917$ for temperatures between 298.15 and 318 K, obtained with the modified TIP5P model. A comparison of the calculated locations of minima and maxima of these distribution functions and those obtained for pure water, along with the corresponding experimental values, is given in Table 2. The simulation results for the three pair potentials do not fully agree with each other nor with the experimental values for pure liquid water. We notice, however, that our results for pure liquid water agree well with the latest experimental data of Soper [27] and of Head-Gordon and Hura [28].

With increasing temperature the first peak of $g_{OO}(r)$ of the xenon solution decreases in height and shifts outward. It is significantly higher than the corresponding peak of pure water under the same thermodynamic conditions (*e.g.*, 3.2 at 298.15 K for the xenon solution, in contrast to 2.9 for pure water), which

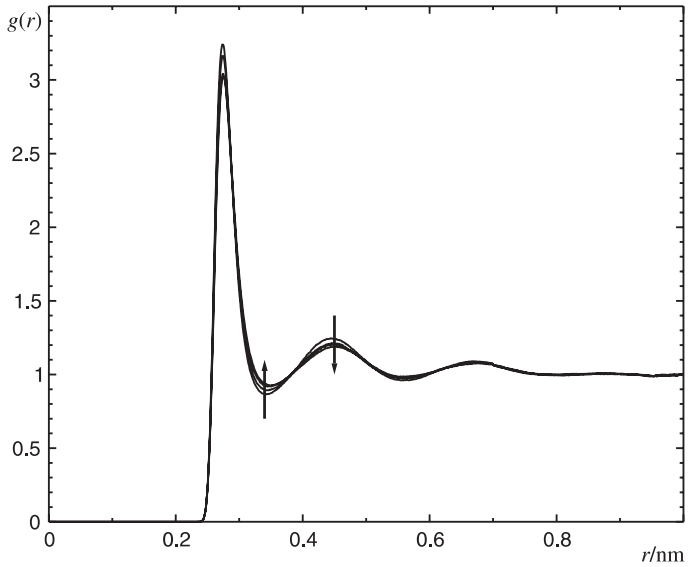

Fig. 1. The oxygen–oxygen radial distribution function of water, $g_{OO}(r)$, in (xenon + water) mixtures with $x_{Xe} = 0.00917$ at 0.1 MPa and 298.15, 313, 323, and 333 K, calculated by Monte Carlo simulation; the arrows indicate increasing temperatures.

indicates a change in the water structure induced by the xenon atoms. This increase is also observed with the SPCE and original TIP5P models for water (Table 2). These results agree with those of Tanaka and Nakanishi [3], who performed simulations for xenon-water solutions using the TIP4P water model and found a $g_{OO}(r)$ first peak location and height of 2.8 Å and 3.1, respectively, which is higher than that of bulk water.

The differences of the heights and widths of the first peak of $g_{OO}(r)$ also point to a change in the coordination number N_c. A coordination number below five indicates that liquid water preserves much of its ice structure, although with differences in hydrogen bonding patterns it might also include deformed hydrogen bonding. Head-Gordon and Hura [28] reported values of 5.1, 5.2 and 4.7 based on the experiments by Narten *et al.* [29], Soper *et al.* [30], and Hura *et al.* [31, 32], respectively. Our value for pure liquid water is 4.7 with the SPCE model and 4.8 with the modified and the original TIP5P models. These results indicate a more structured liquid water, in agreement with the results of Head-Gordon and Hura [28]. In the presence of xenon, however, the coordination number calculated for the first peak of $g_{OO}(r)$ of water increases to 5.2 with the SPCE and modified TIP5P model for water, and to 5.3 with the original TIP5P model, which shows the influence of xenon on the structure and hydrogen bonding pattern of water.

Table 2. Extrema of the oxygen–oxygen radial distribution function of water, $g_{OO}(r)$, for xenon-water solutions with $x_{Xe} = 0.00917$ at 298.15 K and 0.1 MPa and for pure water.

source	1st max.		1st min.		2nd max.		2nd min.		3rd max.	
	r/Å	$g(r)$	r/Å	$g(r)$	r/Å	$g(r)$	r/Å	$g(r)$	r/Å	$g(r)$
simulation results for (xenon + water)										
SPCE [14]	2.8	3.1	3.4	0.9	4.5	1.2	5.6	0.9	6.8	1.1
orig. TIP5P [17]	2.7	3.3	3.4	1.0	4.6	1.2	5.5	0.9	6.7	1.0
opt. TIP5P [19]	2.8	3.2	3.4	0.9	4.5	1.3	5.6	1.0	6.7	1.1
simulation results for pure water										
SPCE [14]	2.9	2.7	3.4	0.8	4.5	1.1	5.5	1.0	6.8	1.0
orig. TIP5P [17]	2.7	2.9	3.4	0.8	4.5	1.2	5.6	0.9	6.7	1.0
opt. TIP5P [19]	2.9	2.9	3.4	0.8	4.5	1.2	5.5	1.0	6.6	1.1
experimental results for pure water										
Narten *et al.* [29]	3.0	2.2	3.5	0.8	4.5	1.2	5.6	0.9	6.9	1.1
Head-Gordon *et al.* [28, 31, 32]	2.7	2.8	3.4	0.8	4.4	1.1	5.5	0.9	6.7	1.1
Soper [27]	2.8	2.2	3.5	0.8	4.5	1.2	5.5	0.9	6.7	1.1

Figures 2 and 3 show the oxygen–hydrogen and hydrogen–hydrogen radial distribution functions, $g_{OH}(r)$ and $g_{HH}(r)$, of water containing xenon. Table 3 lists simulation and experimental results for the peaks of these functions. Evidently, $g_{OH}(r)$ of water changes significantly upon the addition of xenon. The behavior of $g_{HH}(r)$ is similar to that of $g_{OO}(r)$. All these results indicate that the xenon atoms exert an influence on the structure of the surrounding water molecules and on their hydrogen-bonding pattern.

The calculated oxygen–hydrogen coordination numbers in the hydration shell of water are shown in Table 4 for pure water as well as for the water-xenon system. For the latter there is again an increase in comparison to pure water.

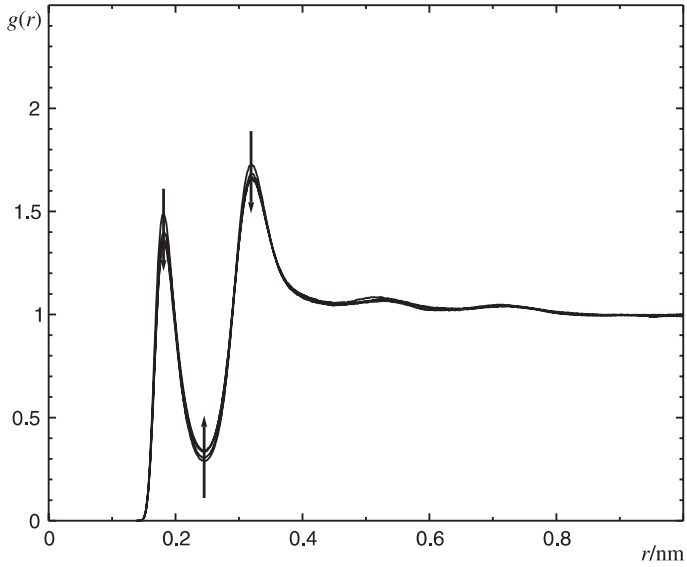

Fig. 2. The oxygen–hydrogen radial distribution function of water, $g_{OH}(r)$, in (xenon + water) mixtures with $x_{Xe} = 0.00917$ at 0.1 MPa, calculated by Monte Carlo simulation. See Fig. 1 for an explanation of the symbols.

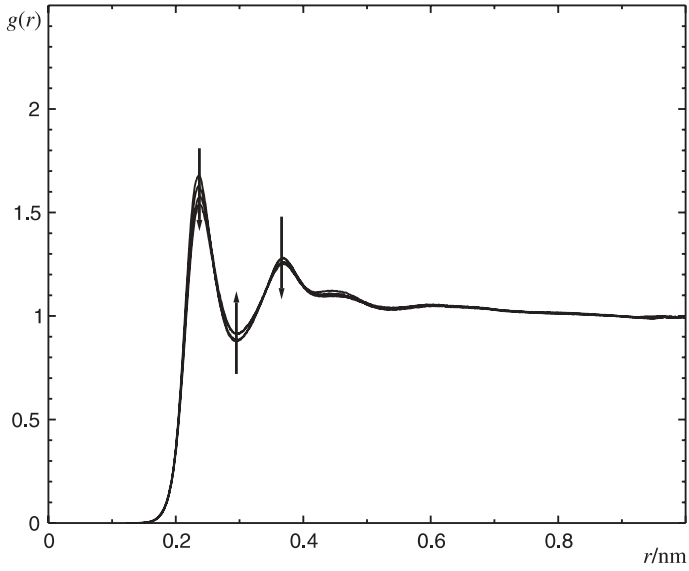

Fig. 3. The hydrogen–hydrogen radial distribution function of water, $g_{HH}(r)$, in (xenon + water) mixtures with $x_{Xe} = 0.00917$ at 0.1 MPa, calculated by Monte Carlo simulation. See Fig. 1 for an explanation of the symbols.

Table 3. Maxima of the oxygen–hydrogen and hydrogen–hydrogen radial distribution functions of water, g_{OH} and g_{HH}, for (xenon + water) mixtures with $x_{Xe} = 0.00917$ and pure water at 298.15 K and 0.1 MPa.

source	$g_{OH}(r)$				$g_{HH}(r)$			
	1st max.		2nd max.		1st max.		2nd max.	
	r/Å	$g(r)$	r/Å	$g(r)$	r/Å	$g(r)$	r/Å	$g(r)$
	simulation results for (xenon + water)							
SPCE [14]	1.8	1.6	3.3	1.8	2.3	1.6	3.7	1.4
orig. TIP5P [17]	1.7	1.6	3.2	1.8	2.4	1.8	3.8	1.3
opt. TIP5P [19]	1.8	1.5	3.2	1.7	2.4	1.7	3.7	1.3
	simulation results for pure water							
SPCE [14]	1.9	1.4	3.5	1.6	2.4	1.8	3.8	1.2
orig. TIP5P [17]	1.9	1.3	3.5	1.8	2.3	1.7	3.8	1.4
opt. TIP5P [19]	1.9	1.3	3.5	1.7	2.3	1.7	3.8	1.3
	experimental results for pure water							
Soper *et al.* [30]	1.9	1.6	3.3	1.5	2.5	1.2	3.9	1.1
Soper [27]	1.8	1.2	3.7	1.3	2.3	1.3	3.8	1.3

Table 4. Hydrogen bonding in the first shell: O–H coordination numbers of (xenon + water) mixtures ($x_{Xe} = 0.00917$) and of pure water for various temperatures.

T/K	$N_{c1,pure}$		$N_{c1,mix}$	
	SPCE	orig. TIP5P / mod. TIP5P	SPCE	orig. TIP5P / mod. TIP5P
298.15	3.3	3.2 / 3.3	3.7	3.9 / 3.8
303	3.2	3.1 / 3.3	3.7	3.8 / 3.7
308	3.2	3.1 / 3.2	3.6	3.7 / 3.7
313	3.2	3.0 / 3.2	3.6	3.7 / 3.7
318	3.1	3.0 / 3.2	3.6	3.7 / 3.6
323			3.5	3.7 / 3.6
328			3.5	3.6 / 3.6
333			3.5	3.5 / 3.6

The original TIP5P model leads to a slightly higher temperature dependence of the coordination numbers for pure liquid water as well as for the water-xenon system than the modified TIP5P and SPCE potential functions. This observation is in agreement with the results of Paschek [2] in which the original TIP5P and the SPCE models for water were used.

Table 5 shows the oxygen–hydrogen coordination number in the second hydration shell for pure water and for the water-xenon system. This number

Table 5. Hydrogen bonding in the second shell: O–H coordination numbers of (xenon + water) mixtures ($x_{Xe} = 0.00917$) and of pure water for various temperatures.

T/K	$N_{c2,pure}$			$N_{c2,mix}$		
	SPCE	orig. TIP5P	mod. TIP5P	SPCE	orig. TIP5P	mod. TIP5P
298.15	6.2	6.3	6.3	5.6	5.8	5.7
303	6.1	6.1	6.0	5.5	5.7	5.7
308	5.9	6.0	5.9	5.4	5.7	5.7
313	5.9	5.8	5.8	5.4	5.6	5.7
318	5.8	5.6	5.7	5.4	5.5	5.6
323				5.3	5.5	5.6
328				5.3	5.4	5.6
333				5.3	5.4	5.5

Table 6. Coordination numbers of xenon in the first and second coordination shells ($x_{Xe} = 0.00917$).

T/K	SPCE		orig. TIP5P		mod. TIP5P	
	N_{c1}	N_{c2}	N_{c1}	N_{c2}	N_{c1}	N_{c2}
298.15	0.38	0.41	0.31	0.46	0.33	0.44
303	0.40	0.38	0.34	0.45	0.35	0.43
308	0.40	0.37	0.37	0.42	0.36	0.39
313	0.41	0.35	0.37	0.40	0.36	0.39
318	0.42	0.34	0.39	0.38	0.36	0.37
323	0.42	0.34	0.40	0.33	0.37	0.35
328	0.42	0.33	0.41	0.30	0.37	0.34
333	0.43	0.31	0.43	0.27	0.37	0.32

decreases with increasing temperature for bulk water as well as for the water-xenon system; the decrease is more pronounced for the original TIP5P water model. In general, these simulation results are in agreement with the nuclear scattering results of Koh *et al.* [33], which show an overall decrease of hydrogen bonding between the water molecules in the vicinity of apolar particles.

Table 6 shows the xenon–xenon coordination number in water over a range of temperatures. The first shell coordination number, N_{c1}, calculated by integrating over the first peak of the radial distribution function, represents contact pairs, whereas the second shell coordination number, N_{c2}, represents solvent-separated pairs. All calculations point to a tendency of xenon atoms to form contact pairs with increasing temperature, which is in agreement with the simulation results of Paschek [2], who observed that contact pairs are stabilized with increasing temperature, whereas solvent-separated xenon pairs become more and more destabilized. Again we notice that the coordination numbers calculated with the original TIP5P model for water show a higher temperature

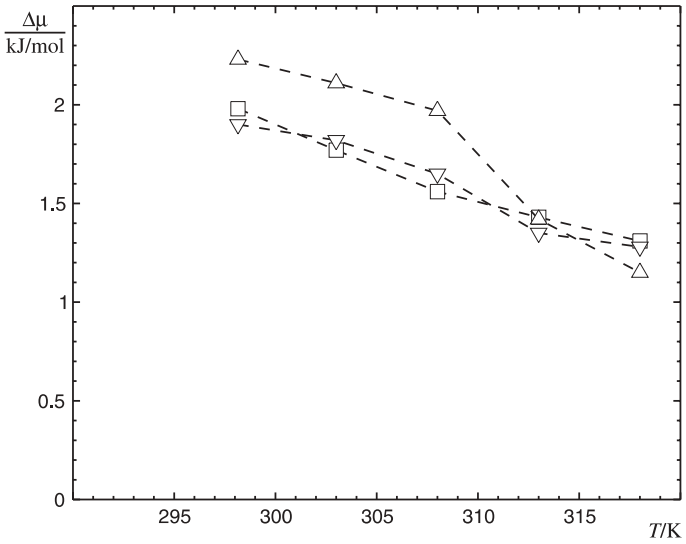

Fig. 4. Change of the chemical potential of liquid water at 0.1 MPa caused by the addition of xenon ($x_{Xe} = 0.00917$). □: SPCE, △: original TIP5P, ▽: modified TIP5P.

dependence than those obtained with the SPCE and modified TIP5P potential functions, which demonstrates the importance of the water pair potential model for studies of hydrophobic interactions.

In our previous study of hydrophobic interactions of methane and ethane molecules in water [19] it was found that, with increasing temperature, both systems tend to form contact pairs. Methane molecules, however, preferably form solvent-separated pairs, even at high temperatures, whereas for ethane contact pairs are more likely. The *quota* of xenon atoms forming contact pairs is higher than those of methane ($N_{c1} = 0.11$ at 298.15 K). This might be due to the difference of cavity sizes between xenon atoms and methane particles, which must have a strong influence on the structural properties of the surrounding water molecules.

In order to show the influence of small amounts of xenon on the thermodynamic properties of water, the change of the chemical potential of water upon addition of the apolar solute at various temperatures is considered:

$$\Delta\mu = \mu_{\text{mix}} - \mu_{\text{pure}} \tag{3}$$

Here μ_{mix} refers to the mixture of 216 water molecules and two xenon atoms studied. For μ_{pure} values from Ref. [19] were used. The results are shown in Fig. 4. The SPCE and the modified TIP5P models give similar trends for the change of chemical potential between 298.15 and 318 K, whereas the original TIP5P model shows a higher temperature dependence.

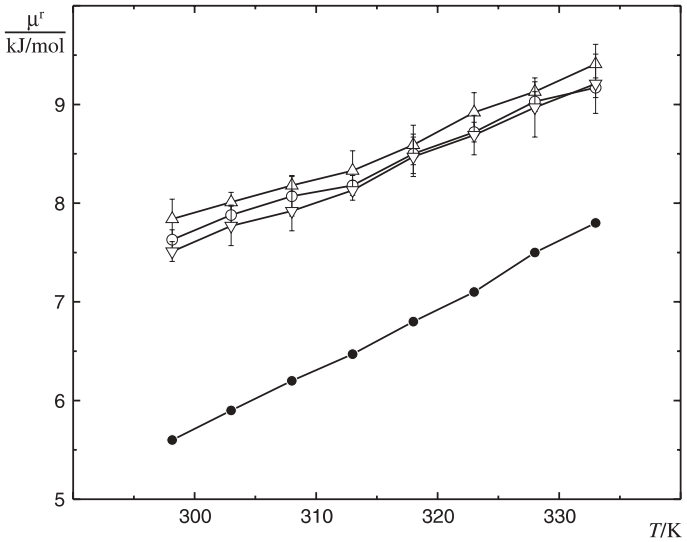

Fig. 5. Residual chemical potential of xenon in water at 0.1 MPa predicted with the SPCE potential for water. ▽: Widom insertion, ○: 2-step deletion, △: Widom deletion method, ●: exp. data [34].

For all three models the residual chemical potential of xenon increases with temperature, which means that the solubility of xenon in water decreases. This tendency was also observed by Paschek for the SPCE potential [2]. Finally it must be noted that, as in our previous study on methane and ethane in water [19], the chemical potentials calculated with the Widom insertion method come closest to the experimental data [34]. Of the three pair potential models for water, the modified TIP5P model gives the best results (see Figs. 5–7).

A comparison of the recent results for xenon in water with previous results for methane and ethane reveals some interesting differences:

1. The first peak of the oxygen–oxygen radial distribution function of xenon solutions is about 17% higher than that of methane solutions, but 12% smaller that that of ethane solutions.
2. The oxygen–hydrogen coordination number in the first shell is also slightly higher for the xenon systems than for the methane systems.
3. In the second shell, the xenon and the ethane systems have oxygen–hydrogen coordination numbers about 9.5% larger than those of the methane system.
4. The change of the chemical potential of water caused by the addition of solute molecules is for ethane twice as large as for methane or xenon.

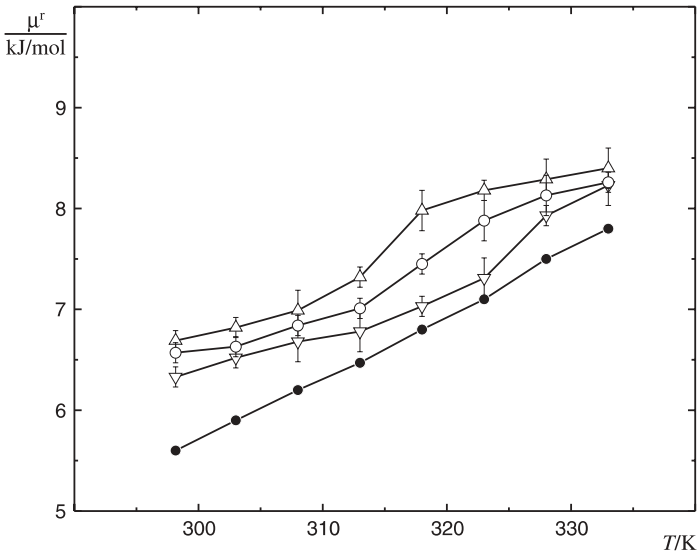

Fig. 6. Residual chemical potential of xenon in water at 0.1 MPa predicted with the original TIP5P potential for water. For an explanation of the symbols see Fig. 5.

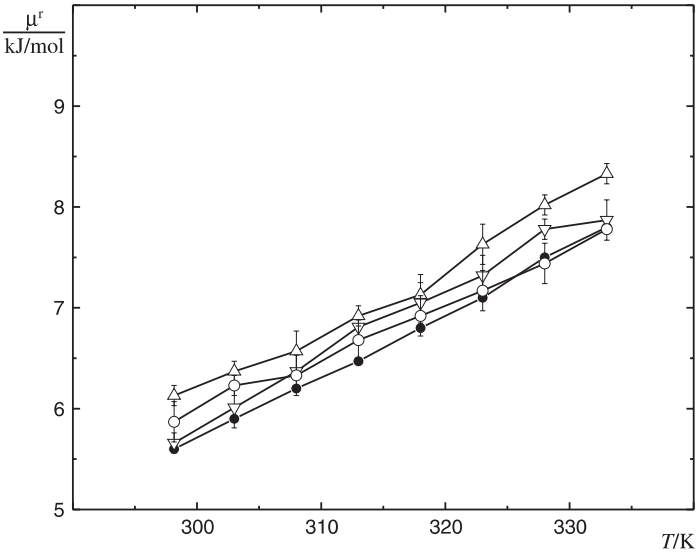

Fig. 7. Residual chemical potential of xenon in water at 0.1 MPa predicted with the modified TIP5P potential for water. For an explanation of the symbols see Fig. 5.

It seems that the chemical potential change depends mostly on the size of the solute molecule (which is similar for methane and xenon), whereas the water structure around a xenon atom differs significantly from that around a methane molecule.

4. Conclusion

The structural and thermodynamic properties of the dilute solutions of xenon in water were studied by NpT Monte Carlo simulations and compared with simulation results for pure water. Three different pair potential functions for water were used: SPCE, original TIP5P, and a modified TIP5P. From the simulations site–site radial distribution functions, average coordination numbers, and residual chemical potentials were obtained.

The structural parameters show that xenon atoms in water show a tendency to aggregate, which becomes more pronounced with increasing temperature. The aggregation leads to contact pairs as well as solvent-separated pairs. The *quota* of the latter decreases with temperature. Similar tendencies had previously been observed for methane and ethane in water; with regard to the ability to form solvent-separated pairs, xenon falls between methane and ethane. It must also be noted that even a small amount of xenon has a significant influence on the site–site radial distribution functions of water.

The chemical potential difference of water shows an approximatively linear dependence on temperature between 298.15 and 318 K. All pair potential models yield residual chemical potentials for water increasing with temperature, but the original TIP5P model shows a stronger temperature dependence. The calculated residual chemical potentials of xenon are in general agreement with experimental data, and the Widom insertion, Widom deletion, and two-step particle deletion methods yield similar trends, although the Widom insertion method usually gives the best results. The pair potential model for water has an influence on the calculated residual chemical potential of xenon; simulation results obtained with the modified TIP5P potential usually come closer to the experimental data than those obtained with the SPCE potential or the original TIP5P potential.

Acknowledgement

Financial support by the Fonds der chemischen Industrie e.V. and INTAS (International Association for the Promotion of Cooperation with Scientists from the New-Independent States of the Former Soviet Union, Project 640-00) are gratefully acknowledged.

References

1. L. R. Pratt and D. Chandler, J. Chem. Phys. **67** (1977) 3683.
2. D. Paschek, J. Chem. Phys. **120** (2004) 6674.

3. H. Tanaka and K. Nakanishi, J. Chem. Phys. **95** (1991) 3719.
4. T. P. Straatsma, H. J. C. Berendsen, and J. P. M. Postma, J. Chem. Phys. **85** (1986) 6720.
5. L. E. S. de Souza and D. Ben-Amotz, J. Chem. Phys. **101** (1994) 9858.
6. I. Ohmine and H. Tanaka, Chem. Rev. **93** (1993) 2545.
7. G. Graziano, J. Chem. Phys. **123** (2005) 034 509.
8. G. Némethy and H. A. Scheraga, J. Chem. Phys. **90** (1962) 3382.
9. H. S. Frank and M. W. Evans, J. Chem. Phys. **13** (1945) 507.
10. M. S. Jhon, J. Grosh, T. Ree, and H. Eyring, J. Chem. Phys. **44** (1966) 1465.
11. H. Popkie, H. Kistenmacher, and E. Clementi, J. Chem. Phys. **59** (1973) 1325.
12. F. H. Stillinger and A. Rahman, J. Chem. Phys. **60** (1974) 1545.
13. H. J. C. Berendsen, J. P. M. Postma, W. F. van Gunsteren, and J. Hermans, in B. Pullman (Ed.), *Intermolecular Forces: Proceedings of the 14th Jerusalem Symposium on Quantum Chemistry and Biochemistry*. Reidel, Dordrecht (1981) pp. 331.
14. H. J. C. Berendsen, J. R. Grigera, and T. P. Straatsma, J. Phys. Chem. **91** (1987) 6269.
15. W. L. Jorgensen, J. Chandrasekhar, J. D. Madura, R. W. Impey, and M. L. Klein, J. Chem. Phys. **79** (1983) 926.
16. W. L. Jorgensen and J. D. Madura, Mol. Phys. **56** (1985) 1381.
17. M. W. Mahoney and W. L. Jorgensen, J. Chem. Phys. **112** (2000) 8909.
18. M. Lísal, J. Kolafa, and I. Nezbeda, J. Chem. Phys. **117** (2002) 8892.
19. O. Coskuner and U. K. Deiters, Z. Phys. Chem. **220** (2006) 349.
20. J. O. Hirschfelder, C. F. Curtiss, and R. B. Bird, *Molecular Theory of Gases and Liquids*. John Wiley, New York (1954).
21. M. P. Allen and D. Tildesley, *Computer Simulation of Liquids*. Clarendon Press, Oxford (1987).
22. D. Frenkel and B. Smit, *Understanding Molecular Simulation*. 2nd edition, Academic Press, London (2002).
23. B. Widom, J. Chem. Phys. **39** (1963) 2808.
24. N. G. Parsonage, J. Chem. Soc. Faraday Trans. **92** (1996) 1129.
25. N. G. Parsonage, Mol. Phys. **89** (1996) 1133.
26. G. C. Boulougouris, I. G. Economou, and D. N. Theodorou, J. Chem. Phys. **115** (2001) 8231.
27. A. K. Soper, Chem. Phys. **258** (2000) 121.
28. T. Head-Gordon and G. Hura, Chem. Rev. **102** (2002) 2651.
29. A. H. Narten, W. E. Thiessen, and L. Blum, Science **217** (1982) 1033.
30. A. K. Soper, F. Bruni, and M. A. Ricci, J. Chem. Phys. **106** (1997) 247.
31. G. Hura, J. M. Sorenson, R. M. Glaeser, and T. Head-Gordon, J. Chem. Phys. **113** (2000) 9140.
32. J. M. Sorenson, G. Hura, R. M. Glaeser, and T. Head-Gordon, J. Chem. Phys. **113** (2000) 9149.
33. C. A. Koh, R. P. Wisbey, X. Wu, R. E. Westmacott, and A. K. Soper, J. Chem. Phys. **113** (2000) 6390.
34. R. Fernández-Prini and R. Crovetto, J. Phys. Chem. Ref. Data **18** (1989) 1231.